Title	Interaction of cell culture with composition effects on the mechanical properties of polycaprolactone-hydroxyapatite scaffolds fabricated via selective laser sintering (SLS)
Author(s)	Eosoly, Szilvia; Vrana, Nihal Engin; Lohfeld, Stefan; Hindie, Mathilde; Looney, Lisa
Publication Date	2012
Publication Information	Eosoly, S, Vrana, NE, Lohfeld, S, Hindie, M ,Looney, L (2012) 'Interaction of cell culture with composition effects on the mechanical properties of polycaprolactone-hydroxyapatite scaffolds fabricated via selective laser sintering (SLS)'. Materials Science & Engineering C-Materials For Biological Applications, 32 :2250-2257.
Publisher	Elsevier
Link to publisher's version	http://www.sciencedirect.com/science/article/pii/S0928493112002883
Item record	http://hdl.handle.net/10379/5522
DOI	http://dx.doi.org/10.1016/j.msec.2012.06.011

Accepted manuscript. Published version: *Materials Science and Engineering: C* 32(8), 12/2012, pp. 2250-2257
DOI: 10.1016/j.msec.2012.06.011

Interaction of cell culture with composition effects on the mechanical properties of polycaprolactone-hydroxyapatite scaffolds fabricated via selective laser sintering (SLS)

Szilvia Eosoly[a], Nihal Engin Vrana[a], Stefan Lohfeld[b], Mathilde Hindie[c], Lisa Looney[a]

[a] Materials Processing Research Centre, Dublin City University, Dublin 9, Ireland
[b] National Centre for Biomedical Engineering Science, National University of Ireland, Galway, Ireland
[c] Université de Cergy Pontoise, Laboratoire de Recherche ERRMECE, Cergy-Pontoise, France

Abstract

In the current study PCL/HA composites were fabricated using SLS as two- and three-dimensional lattice structures and exposed to a cellular component (MC 3T3 osteoblast-like cells). The main aims were to determine the mechanical differences due to powder composition and to observe the physical and mechanical changes pertaining to cell presence. These structures were characterized by compressive mechanical testing, and the effects of cell culturing and degradation on mechanical properties of the scaffolds with different PCL/HA compositions were determined. Moreover, changes in the scaffold morphology due to the cell culture conditions were determined by μ-CT analysis.

Cells steadily grew on the scaffolds for 21 days with preferential distribution around the macropores and initially PCL/HA(15%) composites had higher cell numbers. Removal of loosely sintered parts was observable during the culturing period. Cell culture conditions did not change the compressive moduli significantly but had a distinct effect on compressive strength. For PCL/HA(15%) composites, an initial loss in strength caused by cell culture was reversed by longer cell exposure, with compressive strength of the structures restored to the initial properties ($p \leq 0.05$). μ-CT measurements showed widespread morphological changes in the scaffolds, such as a decrease in the roughness of the struts. In general, in the initial period composites with lower HA content (15 wt.%) showed better metabolic activity compared to the higher HA content, however by day 14 the performance of the two compositions was equal. These results suggest that changes in sintering due to the differences in powder composition can have profound effects on the short and long term mechanical properties of the scaffold particularly under cell culture conditions, and this should be closely considered for SLS processing of scaffolds.

Keywords

SLS; PCL; Hydroxyapatite; Bone; Compressive strength; Osteoblast attachment

1. Introduction

Bone tissue engineering intends to produce patient-specific biological substitutes when natural tissue is damaged or lost. Tissue engineering in general involves developing the relevant tissues into the required form in-vitro by seeding and culturing cells on a 3D scaffold. In the case of bone, the scaffolds aim to mimic the function of the extra-cellular matrix by providing a temporary template for tissue growth. Since bone is an extremely anisotropic composite material, methods that can potentially provide a similar scaffold structure are of utmost interest [1] and [2]. Solid freeform fabrication (SFF) technologies such as selective laser sintering (SLS) have been adapted for fabricating such tissue engineering scaffolds [3], [4] and [5].

Selective laser sintering (SLS) is a powder based SFF technology, which has the potential to fabricate complex geometries with intricate and controllable internal architecture such as those required for bone tissue engineering applications. Furthermore SLS can process bioresorbable polymers and their composites with ceramics.

The manufacturing of such matrices could facilitate good cell penetration and viability overcoming the limitations of conventionally used scaffold fabrication technologies, which include poorly controlled internal features and isotropic properties. To achieve the necessary physical characteristics, composite systems such as polycaprolactone (PCL) with hydroxyapatite (HA) are required. However, the addition of a secondary powder affects the sintering process. The specific composition of the powder mix results in scaffolds with different microscopical properties, which in turn may also be modified in a different way when exposed to cells. Both the extent of sintering and biological action can influence mechanical properties, but very little is understood about how these effects combine.

An SLS system consists of a powder bed flanked on each side by powder supply beds and a laser source above. The laser beam is positioned by the movement of two mirrors, and selectively scans the surface of the powder bed. Its movement is controlled according to the data file containing the 2D geometry of a slice of the required 3D shape. The interaction of the laser beam with the powder raises the temperature of the powder particles to their melting point, resulting in sintering or fusion of the neighboring particles. When one layer is sintered, the powder supply bed is raised, the powder bed is lowered and a new layer of powder is deposited on the top of the powder bed by a roller. The sintering process is repeated until the 3D part is completed. Challenges in adopting SLS technology for scaffold manufacture relate to the small scale of required features, replicating the bone's mechanical properties and getting the right porosities and surface characteristics.

The composition of the powder mix and processing parameters are the controllable inputs. In addition, there are two main approaches used to produce porosity by SLS. One exploits the fact that SLS is a powder based process, which intrinsically induces porosity in the ‘solid’ designed parts. Using this method Chua et al. [6] successfully produced PVA scaffold geometries with intrinsic porosity containing up to 30 wt.% HA [6]. Bioactivity analysis of scaffolds was carried out in simulated body fluid, and hydroxyl-carbonate-apatite formation was observed on the scaffold surface. Sintering parameters for PVA–HA (21.5 wt.%) were improved in a study by Wiria et al. [7]. Tan et al. [8] found the process parameter windows for fabricating scaffolds using PVA, PCL and PLLA. Wiria et al. [9] manufactured scaffolds of PCL and its composites with HA of different morphology. Mechanical properties of fabricated parts were reported and were in the range of trabecular bone. In a more

recent study PLG (poly-l-lactide-co-glycolide) and its composites with HA and HA–TCP blend were examined for SLS fabrication. The HA composites resulted in poor sintering, presumably due to small particle size (below 14 μm) that hindered the sinter process by 'insulating' the PLG particles [10]. SLS processing of biocompatible but not bioresorbable polymeric powder composites (such as polyethylene/HA) has been done by Hao et al. [12] and by Zhang et al. [11] and [12]. Most of their work was carried out using PEEK or PA, however these materials are not bioresorbable.

The second approach is to design a specific inner geometry with pores, as well as the outer shape of the scaffold. This method has been less extensively studied, but offers the best opportunity to exploit the benefits of the process over alternatives. Williams et al. [2] manufactured PCL scaffolds with 3D orthogonal channels with designed pores ranging between 1.75 and 2.5 mm. The SLS parameter settings for this PCL were optimized by Partee et al. [13]. In a more recent study [14], 2D lattice structures were fabricated from PLLA/HA microspheres.

The results of several research groups demonstrate that PCL/HA composites are viable materials for fabrication of bone scaffolds [15], [16], [17] and [18]. However, during degradation bioresorbable polyesters such as the poly-lactic acid (PLA) can release degradation products that reduce local pH, which accelerates degradation and induces inflammatory reactions [19]. The addition of HA is known to compensate this acidic release through the presence of alkaline calcium phosphate [20]. Degradation and resorption kinetics of PCL are considerably slower than other polyesters, due to its hydrophobic character and high crystallinity. Sun et al. showed that in vivo PCL degrades over a period of 2 years, and its degradation products are metabolized and ultimately excreted from the body [21] and [22]. Oh et al. reported no adverse tissue reactions when examining PCL implants in vivo [22].

The addition of HA is considered beneficial, since it reduces hydrophobicity of the polymer, therefore it is more favorable for cell attachment, and accelerates degradation [23]. Nevertheless, there are conflicting short-term results reported in literature about the effect of HA addition to PCL composites in terms of cell attachment, proliferation and differentiation. Some authors claim that the presence of HA in PCL scaffolds has little or no effect on biological response [4], [24], [25] and [26]. Others have shown that scaffolds with 25 wt.% of HA demonstrate improved cell differentiation compared to PCL scaffolds [27]. HA undergoes degradation under in-vivo conditions [28]. This gradual dissolution releases calcium and phosphate ions that can potentially influence nearby cell populations, and may enhance bone cell mineralization and bonding to the surrounding tissue. There is much more to be understood about this interaction. In the current study the effect on cell response of two HA compositions (15 wt.% and 30 wt.%) with designed scaffold porosity is compared. Scaffold shapes and compositions were chosen based on a previous work [29].

In addition to the influence of material composition on cells, the activities of cells on biodegradable scaffolds can be strong enough to change the surface characteristics and mechanical properties of the scaffold [30]. As SLS technology offers pre-defined structures regardless of the powder composition; it is the ideal medium to evaluate the corresponding effects of cells and powder composition on the mechanical properties of the final structure during a predefined culture time.

In this study, scaffold geometries were selective laser sintered from PCL and its composites with HA with the objective to examine the effect of HA addition on surface roughness, wettability, mechanical behavior and surface morphology and MC 3T3 osteoblast like cells' activity. Changes

induced by the presence of cells with respect to material composition were verified by means of µCT analysis, biomechanical tests and bioactivity assays.

2. Materials and methods

2.1. Materials

For SLS processing, polymers in powder form are needed. Polycaprolactone (PCL) is not commercially available as powder, but is sold in the form of ~ 3 mm pellets. These were purchased from Sigma Aldrich Chemical Co. (catalog no. 440744), and cryogenically ground by Solid Composites Ltd., Germany. The fraction of the resulting powder below 100 µm was used for SLS. Its morphology and particle size distribution are presented in Fig. 1A and C, respectively.

The hydroxyapatite (HA) powder (Fig. 1B) used in the experiments was sold under the brand name Captal 60-1 (Plasma Biotal Ltd.). Supplier data indicates an average particle size of 45 ± 5 µm and bulk density of 1.3 g/cm3. PCL/HA powder blends containing 15 and 30 wt.% of HA for SLS processing were produced by physical blending in a v-blender for 30 min at 40 rpm. (Accordingly, the labels PCL/15HA and PCL/30HA were used.)

2.2. Fabrication of scaffolds

All specimens for SLS fabrication were designed using Pro/ENGINEER® and were exported into STL file format. The geometry was built from simple cubic elements and is shown in Fig. 2. Designed strut thickness is 0.6 mm and designed pore size is 1.2 mm. Cubic samples for compression testing are 9.6 × 9.6 × 6 mm, while lattice layers are 9.6 × 6 × 2 mm. For contact angle and surface roughness measurements solid disks were designed and fabricated with intrinsic microporosity.

All samples were manufactured on a DTM Sinterstation 2500plus (3D Systems, Valencia, CA) installed with a low power (25 W), λ = 10.6 µm continuous wave CO_2 laser focused to a 400 µm spot. For processing PCL and its composites, the size of the powder bed and the feed bed was reduced, so that the machine could operate using smaller amounts of powder.

Process parameters were set via DTM's Build Setup interface. In the software, DuraForm (polyamide) powder was selected as the material used, its recommended parameter settings were loaded into the software and individual process parameters were changed to enable processing of PCL powder. The following parameters were used to fabricate the PCL and PCL composite lattices: laser fill power of 10 W, outline laser power of 5 W, scan spacing of 0.15 mm, layer thickness of 0.15 mm, and part bed temperature of 38 °C. The default values for outline and fill scan speed were 1778 mm/s and 5080 mm/s respectively [31].

Once parts were manufactured, an extra 2 mm of the powder was deposited to allow for part cooling without significant thermal gradients within the powder bed. When the powder bed cooled down to room temperature, parts were removed and excess powder was brushed off from the exterior and the inside was cleaned using compressed air.

2.3. Characterization of scaffolds

Compressive mechanical properties of the fabricated and cell seeded lattice structures were tested according to ISO 604 standards using a 5 kN load cell at a crosshead speed of 1 mm/min and with a 1 N preload. A flat plate was used to apply a uniformly distributed load on a Zwick/Roell universal

testing machine. Compressive modulus, and compressive yield strength values were obtained using Zwick/Roell Text Expert II software. All testing was carried out at room temperature.

Surface morphology of the sintered parts was examined using a Zeiss EVO LS15 SEM. Samples were gold coated and examined under high vacuum.

Surface profile was obtained using an optoNCDT laser profiler. Obtained data was analyzed in Matlab 7.5.1 and surface roughness (Ra) was calculated.

2.4. Bioactivity

To expose scaffolds to the action of degradation, fabricated samples were transferred to 24 well plates with sterile forceps. Samples were sterilized with 70% ethyl alcohol for 2 h and then alcohol was washed away by several copious washes with sterile PBS (phosphate buffered saline). Samples were suspended in 2 mL sterile PBS (10 mM, pH 7.4) and then incubated under standard tissue culture conditions (37 °C and 5% CO_2). The degradation medium was changed aseptically weekly. After 1 week of incubation, samples were removed, washed with copious amount of distilled water, blotted dry and were compression tested (n = 3).

For determination of cell attachment; MC 3T3 mouse calvarial osteoblast cells were cultured under standard tissue culture conditions (37 °C, 5% CO_2) in alpha-MEM medium (Gibco, USA) supplemented with 10% fetal bovine serum and 1% penicillin/streptomycin. All experiments were conducted with cells between passages 4 and 8. Samples were sterilized by immersing them in 70% ethyl alcohol for 2 h and then washed with sterile PBS. Samples were stored in culture medium in a CO_2 incubator overnight to promote protein adsorption. The cells were trypsinized and the cell number was quantified by tryphan blue and then seeded onto samples, at a concentration of 1×10^5 cells/cm^2 in 20 µL of the medium. After an initial attachment period, the medium was completed to 500 µL.

To assess cell attachment and morphology; samples were stained with DNA binding fluorescent reagent DAPI and FITC-labeled phalloidin. Samples were fixed with 3.7% formaldehyde for 5 min and then rinsed with PBS. Afterward cells were permeabilized by treatment with 0.1% Triton-X solution. After removal of Triton-X; samples were incubated in 1% PBS–BSA solution at 37 °C for 30 min to decrease non-specific absorption of the dyes. Afterward 1:1000 dilution of DAPI and 1:200 dilution of FITC-phalloidin were applied to the samples and the samples were incubated in the dark for 15 min. After washing with copious amount of PBS, the samples were observed under an epifluorescence microscope under single or multiple fluorescence modes (Olympus, Japan).

Cell proliferation was quantified by Alamar blue cell proliferation assay (AbBiotech, USA) at 7 days, 14 days and 21 days post seeding. Alamar blue solution (10% in serum free alpha MEM medium) was applied onto the samples and absorbance of the dye at 562 and 595 nm, was determined after 1 h of incubation in culture. Absorbance readings were converted to dye reduction % as per instructions of the provider. Dye reduction (%) is indicative of cellular metabolic activity, i.e. higher reduction signifies a higher cell number. All experiments were done 3 times independently with a minimum sample number ≥ 3.

Alkaline phosphatase (ALP) assay (n = 3) was performed with cells cultured for 7 days and 14 days with the medium containing 100 µM ascorbic acid, and 10 mM glycerophosphate, on scaffolds, using

a Sensolyte® pNPP alkaline phosphatase assay kit (AnaSpec, USA). Briefly, cells were detached from scaffolds in a 500 µL lysis buffer, provided in the kit, for 20 min with an ultrasound bath. Lysates were centrifuged for 10 min at 2500 g at 4 °C and the supernatant was collected for ALP assay using p-nitrophenyl phosphate as the substrate. ALP provided in the kit was used as a standard, and results were normalized to the amounts of total protein measured with the Bradford assay.

2.5. µ-Computer tomography (µCT)

Both empty and cell seeded samples were scanned using µ-computer tomography (µCT) (Phoenix Nanotom 180 kV Nanofocus System) at the Waterford Institute of Technology. The limiting resolution is between 1 and 5 µm and depends on the operating voltage (30–300 kV) using a 50 kV x-ray tube voltage and 140 µA current with 500 ms detector exposure and 1152 × 1152 pixel detector size.

2.6. Contact angle

The contact angle of water on the sintered surfaces was measured using an ArtCAM 130 MI BW monochrome camera, and FTA200 contact angle analyzer software. The static sessile drop method was used to analyze the initial contact angle.

2.7. Statistical analysis

The level of statistical significance was defined for each analysis in the relevant figure ($p < 0.1$, $p < 0.05$ and $p < 0.01$); analyses were done with ANOVA.

3. Results

Fabricated samples exhibit a double porous structure by having a designed macroporous architecture and a microporous structure (formed due to the processing method) within the struts. Fabricated samples were subjected to compressive loading and failure mechanisms were examined by SEM. As Fig. 4 shows failure of the scaffolds occurred by buckling of the load bearing (z) struts while plastic hinges were formed either around the conjunction of the struts, or along the unevenly deposited layers and finally, at high strains, layers shifted on each other when the hinges failed. The mechanical properties of samples with different compositions were also tested after degradation tests and cell culturing.

Fig. 5A–B shows that the degradation test resulted in a slight decrease in compressive strength in all cases, however the decrease was only significant in the case of the scaffolds containing 30 wt.% HA; indicating that the main material loss is due to unsintered HA. During the degradation test HA particles trapped inside or loosely connected to the structure of the struts were detached and washed off. Therefore its effect became more measurable with increasing HA content, and the resulting poor incorporation of the ceramic. In the case of the PCL samples cell culturing for 1 week resulted in further loss of compressive strength, however after the second week the strength reached the strength of the control samples. For samples containing 15 wt.% HA an intense improvement was observed just after 1 week, that was maintained for the second week as well. In the case of the scaffolds containing 30 wt.% HA the enhancement was only significant after the second week. These results were in good agreement with the obtained Alamar blue results. The results of the Alamar blue assay indicated that during the first 7-day period extensive cell colonization of the 15 wt.% HA scaffold occurred, that somewhat slowed down in the second week

compared to the increase in the other two samples (Fig. 6). Data in Fig. 6 showed a statistically significant difference ($p < 0.05$) in the cell numbers over the cultured time. An active proliferation period was seen on the samples; cell numbers increased over time until day 21 when they reached a plateau for all material compositions. In general, composites with lower HA content (15 wt.%) showed higher cell numbers compared to the higher HA content. In the first 7-day period, PCL/15 wt.% HA samples performed significantly better in terms of bioactivity.

To further understand the interaction of cells with the fabricated scaffolds, adhesion and proliferation of osteoblasts were evidenced through SEM, and fluorescence microscopy. Cell adhesion was pronounced around the designed macropores and spread cells were observed at various depths after 7 days (Fig. 7A–B). SEM images also confirmed that cells covered the surface of the macroporous PCL as well as its composites with HA. Two days after cell seeding, cells were spread on the particulate surface especially around the pore areas (Fig. 7C). With fluorescent microscopy images, cells were observed both on the surface and also with directionalities going deeper into the micropores of the polymeric matrix suggesting cell migration into the scaffold. The formation of a cell layer on the selective laser sintered composites supports significant proliferation of adhered cells. Cells were observed on rough surfaces with Ra between 30 and 40 μm, which might affect their ability to adhere and spread; however quantification of surface roughness showed that there was no significant difference between different groups (Table 1) and the surface roughness was not one of the determinants of the cell behavior for this case.

Besides surface roughness, hydrophilicity of the scaffold surface is also a necessary consideration for cell attachment and proliferation. The initial contact angle of pure PCL scaffolds was 104 ± 5.5° indicating a hydrophobic surface. This was consistently decreased by the addition of HA. The initial contact angle for composites with 15 wt.% of HA decreased to 98 ± 13.6° and with 30 wt.% HA to 83 ± 16.9°. At the $p < 0.05$ significance level, only the difference between pure PCL and 30 wt.% HA was statistically significant. Results demonstrated the ability of the added HA powder to reduce hydrophobicity of the PCL scaffolds. Large variations measured for the same compositions are due to inhomogeneous distribution of HA particles on the micron scale and to the rough surface created by the manufacturing technology.

One concern with 3D matrices is whether cells are able to migrate into the full depth of the scaffold and how this would affect the scaffold. To reveal changes induced by cells and cell culture conditions within the micropores of the struts of the scaffolds, i.e. on the morphology of the scaffolds μCT was used. Fig. 8A and B shows reconstructed scaffolds in 3D, indicating the changes in the internal architecture of the struts following exposure to the cell medium. The surface morphology of the particles of the as-sintered scaffold is more irregular and edgy, and particle boundaries are easily distinguishable. After 1 week of incubation with cells the loosely connected particles were washed off from the struts and the surface of the scaffolds became slightly smoother, and since cells covered the surface particle boundaries are not visible. Structural changes in struts can be inferred on the seeded scaffolds marked by the higher intensity areas (bright white areas) in Fig. 8B. The cross sections of the scaffolds were also examined to confirm the changes within the microstructure of the struts (Fig. 3). A set of representative slices are shown in Fig. 9 to demonstrate the significant structural and architectural changes of the scaffold after cell culturing. In the case of the unseeded samples two phases were present in the images: scaffold (bright), and air (dark), while in the case of the cell seeded structures three phases were evident: modified scaffold (bright), scaffold (medium),

and air (dark). The average width of the struts was around 800 μm, therefore these cross sectional images imply that cells penetrated ~ 400 μm into the microstructure of the struts composing the macrostructure of the 9.6 × 9.6 × 6 mm scaffold.

To see whether the strength increase in composites is related to mineralization alkaline phosphate (ALP) activity was quantified at the relevant time points. It has been previously shown by Shor et al. and Ciapetti et al. [32] that compared to pure PCL scaffolds, ALP activity on HA reinforced PCL scaffolds gives higher scores. In the current study therefore, only the two HA levels were compared after both 7 and 14 days of cell culturing. Results of the experiments show that after 1 week of culturing ALP activity on scaffolds containing 15 wt.% HA scores higher values (0.204 ± 0.032 ng ALP/μg protein vs. 0.143 ± 0.029 ng ALP/μg protein). However, by day 14 the difference between the two is not detectable (0.290 ± 0.050 ng ALP/μg protein vs. 0.335 ± 0.137 ng ALP/μg protein). This is in good agreement with the results of the mechanical tests, where the difference was significantly better on scaffolds containing 15 wt.% HA during the initial 7-day period, by day 14 the difference was insignificant.

4. Discussion

Previous work on the PCL–HA biphasic mostly focused on the effect of HA or PCL presence on cell activities. The current work is focused on the mechanical property changes in a highly anisotropic and porous structure with different compositions in the presence of osteoblastic cells. Since bone structure is highly oriented and needs to bear load, examination of anisotropic structures during remodeling provides important information for different SSF production methodologies.

Macroporosity of the scaffolds was defined, and tailored by the designed CAD models while microporosity within the struts of the structures was guided by SLS process parameters and by the morphology of the powder. The presence of an interconnected microporosity throughout the struts was beneficial for cellular integration as penetration of cells throughout the 553 mm3 scaffold was evidenced by fluorescent microscopy (Fig. 7) and μCT slice data (Fig. 9).

The addition of the HA phase did not change the surface roughness of the scaffolds however it made the surface significantly more hydrophilic and therefore more bioactive and favorable for cell attachment as it has been demonstrated by the Alamar blue and the ALP results for the composition with 15 wt.% HA content. It is assumed that sintering of the scaffolds with 30 wt.% HA content was looser and therefore during the degradation tests and cell culturing a significant amount of the loosely integrated HA particles were disintegrated from the structure and washed off. That explains the lack of improvement of bioactivity in these samples compared to the control samples. Results of mechanical testing also support this hypothesis, as scaffold structures with 30 wt.% HA content were significantly weaker.

It has been observed in previous experiments [29] that the effect of HA addition on the mechanical properties of the control samples is dependent on how strong the sintering is among the polymer particles. When sintering of the polymer results in good integrity, HA particles could limit molecular motion in PCL, resulting in increased compressive modulus. However, when sintering of the polymer was weak HA particles could not properly integrate into the polymer particles, and remained partly exposed to the surface, therefore, HA addition induced inferior mechanical properties. As described above, failure of the scaffolds subjected to compressive loading occurred by buckling and hinge

formation (Fig. 4). Hinge formation is facilitated by delamination or shifting of formed layers normal to loading. As the HA content of the composition increased the delamination/layer shifting problem became more apparent as the HA particles acted as insulating agents working against coherent sintering within layers, and against cohesion between layers. As no force is applied during sintering to help the adherence of consecutive layers, proper melting of the particles is a key. The problem can be overcome by optimization of process parameters for each material composition. The current research therefore does not aim at comparing the three examined compositions, but instead examining the effect of cell culturing conditions on each composition.

Aside from the direct effects on the mechanical properties, the initial composition could affect the response of the cells to the scaffolds; hence it can indirectly affect the final mechanical properties. However in the current study, the compressive moduli of the samples were only slightly influenced by the degradation test and cell culturing. Fig. 5A–B shows these effects for scaffolds with different compositions. A control sample is included in the graphs for all three compositions. Overall, the compressive strength was negatively altered with the degradation test (Fig. 5), however after 2 weeks of cell culture, cultured cells integrated into the scaffold and increased its overall strength, its value reached the initial compressive strength of the untreated scaffolds (controls) in all cases. Alamar blue results were in good agreement with this as bioactivity of the samples with low 15 wt.% HA content was higher than that of 30 wt.% during the first 2 weeks, and by day 21 there was no significant difference between bioactivities of the different compositions.

The addition of HA to PCL is still favorable, since the degradation time of PCL is over 2 years, and that the degradation rate is profoundly increased by the presence of HA particles [21] and [23].

Previous studies suggested that modulus is a good indicator for the degree of mineralization and toughness is a good predictor for type-I collagen formation [33] and [34]. In the current study the elastic moduli of the samples were measured and have not been significantly altered by the degradation test or cell culturing experiments, unlike the findings of Erisken et al. when examining the tensile properties of electrospun PCL/TCP meshes seeded with MC 3T3-E1 cells after 1 and 4 weeks of cell culturing in 2D [35]. The authors observed a slight, but statistically significant increase in modulus after the first week and a two-fold increase after 4 weeks indicating a modest mineralization after 1 week and a significant high degree mineralization after 4 weeks. The 2-week culturing period in the current experiment was selected to check if similar results can be obtained in a shorter term. Although in the present case compressive properties were examined, a similar tendency was expected. However it has to be pointed out that in the Erisken experiment the samples were thinner (they were only 2D meshes), while in the current case 3D structures with a height of 6 mm were seeded. Therefore, the results presented here, can be due to a number of reasons: i) lower effective cell seeding surface and ii) cells might not have penetrated throughout the 6 mm height of the scaffold, and it is possible that while cell activity is prominent in some areas of the sample, degradation takes place in others if the cells have not reached that area. These results showed that even though addition of HA into the powder mix caused initial decreases in mechanical properties, the increased cellular activity due to its presence made up for the loss, especially for the 15 wt.% composition.

The data available in literature on the effect of HA presence on bioactivity is highly contradictory. For example, Shor et al. [20] demonstrated that scaffolds with 25 wt.% HA exhibit improved cell

activity compared to pure PCL scaffolds fabricated via precision extrusion deposition. Although, Alamar blue assay showed no statistical difference between PCL and PCL/HA, PCL–HA scaffolds had a significantly higher ALP activity. On the other hand, it was observed by several groups that the presence of HA in the PCL scaffolds only slightly affects biological response. Comparing FDM fabricated PCL and PCL/HA scaffolds seeded with human marrow mesenchymal stem cells, Endres et al. [36] found that initially cells in the PCL–HA scaffolds showed less metabolic activity, but reached the same level as PCL by day 28. Chim et al. [4] also reported no significant difference between PCL and PCL/HA scaffolds fabricated by FDM when using human calvarial osteoblast. Ciapetti et al. [32] tested PCL and PCL/HA (40 wt.%) scaffolds prepared by phase inversion and casting technique, and it was found that when examining the metabolic activity of Saos-2 cells, the HA reinforced samples scored higher values compared to pure PCL. The same was observed for the release of ALP, HA reinforced samples demonstrated a higher ALP release, which reached a detectable amount in cultures at 7 days from seeding. Causa et al. [37] examined the Saos-2 cell response of different compositions of PCL/HA composites (13 and 32 vol.% HA) fabricated via phase inversion and casting technique. The release of ALP was higher for cells grown in PCL/13 vol.% HA. This trend was confirmed with human osteoblasts (hOB) (tested on compositions of 13, 20, 32 vol.% HA). Osteoblasts on PCL/32 vol.% HA never reached the ALP levels measured for the other scaffolds. Cells on PCL/32 vol.% HA grew slowly and showed a less differentiated phenotype during growth of the scaffold.

Previous studies also showed that the addition of HA to PCL does not result in a significant increase in cell numbers. This was structure independent as this observation was made for foams [38], films [39] and surface coatings [40]. The composition has indirect effects such as changes in the localization of the cells due to differences in surface properties. But these effects are generally not strong enough to alter cellular proliferation significantly. However, they can have stronger effects on osteoblast phenotype and scaffold mineralization. Current literature supports the proposition that addition of an intermediate level of HA can be beneficial, as observed in the current study. Moreover, current results together with previous studies suggest that, the actual determinant on cell activity of the composite systems is the production method; i.e. the mode of presentation of HA and polymer to the cells and the SFF system selective laser sintering which provides a strong platform to observe these effects in a highly controlled 3D environment.

5. Conclusions

This study primarily investigated the effect of cell culturing and material composition on the surface morphology and mechanical properties of selective laser sintered scaffolds. The effects were composition dependent and the results in the current study show that addition of HA into fabricated scaffolds can have beneficial effects for their bioactivity. Changes in mechanical properties were examined with respect to cell culturing conditions and as an indicator of cell integration and activity. The elastic moduli of the samples of any composition have not been significantly altered by the degradation test or cell culturing experiments. Overall, the compressive strength was negatively altered with the degradation test, however after 2 weeks of cell culture, its value reached the strength of the untreated scaffolds in all cases.

Surface roughness of the scaffolds was not significantly altered by addition of the ceramic phase, while it reduced hydrophobicity of fabricated scaffold surfaces. Qualitative analysis by µCT showed that the surface of the designed scaffold architecture was smoothened by the culturing conditions.

Proliferation of adhered cells, and formation of a cell layer on the selective laser sintered composites were observed and osteoblasts were also encapsulated within the micropores of the struts. The cross sectional images from µCT confirm a remodeling of up to ~ 400 µm into the microstructure of the struts. Alamar blue and ALP activity assays revealed, that in general, in the initial period composites with lower HA content (15 wt.%) showed better metabolic activity compared to the higher HA content, however by day 14 the performance of the two compositions was equal.

The current bioactivity results imply that there is a need to find an optimum HA percentage that would optimize bioactivity and mechanical property gains. This will require utilization of design of experiment methodologies such as those used to optimize the processing parameters for scaffold manufacturing [13] and [29].

Acknowledgments

This research has been supported by a Marie Curie Early Stage Research Training Fellowship of the European Community's Sixth Framework Programme under contract number MEST-CT-2005-020621.

References

[1] G. Wei, P.X. Ma. Biomaterials, 25 (2004), pp. 4749–4757

[2] J.M. Williams, A. Adewunmi, R.M. Schek, C.L. Flanagan, P.H. Krebsbach, S.E. Feinberg, S.J. Hollister, S. Das. Biomaterials, 26 (2005), pp. 4817–4827

[3] W.-Y. Yeong, C.-K. Chua, K.-F. Leong, M. Chandrasekaran. Trends Biotechnol., 22 (2004), pp. 643–652

[4] H. Chim, D.W. Hutmacher, A.M. Chou, A.L. Oliveira, R.L. Reis, T.C. Lim, J.T. Schantz. Int. J. Oral Maxillofac. Surg., 35 (2006), pp. 928–934

[5] E. Sachlos, J. Czernuszka. Eur. Cells Mater., 5 (2003), pp. 29–39

[6] C.K. Chua, K.F. Leong, K.H. Tan, F.E. Wiria, C.M. Cheah. J. Mater. Sci. Mater. Med., 15 (2004), pp. 1113–1121

[7] F. Wiria, C. Chua, K. Leong, Z. Quah, M. Chandrasekaran, M. Lee. J. Mater. Sci. Mater. Med., 19 (2008), pp. 989–996

[8] K.H. Tan, C.K. Chua, K.F. Leong, C.M. Cheah, W.S. Gui, W.S. Tan, F.E. Wiria. Bio-Med. Mater. Eng., 15 (2005), pp. 113–124

[9] F.E. Wiria, K.F. Leong, C.K. Chua, Y. Liu. Acta Biomater., 3 (2007), pp. 1–12

[10] R.L. Simpson, F.E. Wiria, A.A. Amis, C.K. Chua, K.F. Leong, U.N. Hansen, M. Chandrasekaran, M.W. Lee. J. Biomed. Mater. Res. Part B Appl. Biomater., 84B (2008), pp. 17–25

[11] Y. Zhang, L. Hao, M.M. Savalani, R.A. Harris, L.D. Silvio, K.E. Tanner. J. Biomed. Mater. Res. Part A, 91A (2009), pp. 1018–1027

[12] L. Hao, M. Savalani, Y. Zhang, K. Tanner, R. Harris. Proc. Inst. Mech. Eng. Part H J. Eng. Med., 220 (2006), pp. 521–531

[13] B. Partee, S.J. Hollister, S. Das. J. Manuf. Sci. Eng., 128 (2006), pp. 531–540

[14] W. Zhou, S. Lee, M. Wang, W. Cheung, W. Ip. J. Mater. Sci. Mater. Med., 19 (2008), pp. 2535–2540

[15] P. Yilgor, R.A. Sousa, R.L. Reis, N. Hasirci, V. Hasirci. Macromol. Symp., 269 (2008), pp. 92–99

[16] Y. Wang, L. Liu, S. Guo. Polym. Degrad. Stab., 95 (2010), pp. 207–213

[17] S. Fuchs, X. Jiang, I. Gotman, C. Makarov, H. Schmidt, E.Y. Gutmanas, C.J. Kirkpatrick. Acta Biomater., 6 (2010), pp. 3169–3177

[18] J. Zhao, K. Duan, J.W. Zhang, X. Lu, J. Weng. Appl. Surf. Sci., 256 (2010), pp. 4586–4590

[19] H.-Y. Cheung, K.-T. Lau, T.-P. Lu, D. Hui. Compos. Part B Eng., 38 (2007), pp. 291–300

[20] W. Linhart, F. Peters, W. Lehmann, K. Schwarz, A.F. Schilling, M. Amling, J.M. Rueger, M. Epple. J. Biomed. Mater. Res., 54 (2001), pp. 162–171

[21] H. Sun, L. Mei, C. Song, X. Cui, P. Wang. Biomaterials, 27 (2006), pp. 1735–1740

[22] S.H. Oh, I.K. Park, J.M. Kim, J.H. Lee. Biomaterials, 28 (2007), pp. 1664–1671

[23] J. Chlopek, A. Morawska-Chochol, C. Paluszkiewicz, J. Jaworska, J. Kasperczyk, P. Dobrzyński. Polym. Degrad. Stab., 94 (2009), pp. 1479–1485

[24] F.C. Vincenzo Guarino, Paolo A. Netti, Gabriela Ciapetti, Stefania Pagani, Desiree Martini, Nicola Baldini, Luigi Ambrosio. J. Biomed. Mater. Res. Part B Appl. Biomater., 86B (2008), pp. 548–557

[25] M. Endres, D. Hutmacher, A. Salgado, C. Kaps, J. Ringe, R. Reis, M. Sittinger, A. Brandwood, J. Schantz. Tissue Eng., 9 (2003), pp. 689–702

[26] B. Caulfield, P.E. McHugh, S. Lohfeld. J. Mater. Process. Technol., 182 (2007), pp. 477–488

[27] L. Shor, S. Güçeri, X. Wen, M. Gandhi, W. Sun. Biomaterials, 28 (2007), pp. 5291–5297

[28] K. Hyakuna, T. Yamamuro, Y. Kotoura, M. Oka, T. Nakamura, T. Kitsugi, T. Kokubo, H. Kushitani. J. Biomed. Mater. Res., 24 (1990), pp. 471–488

[29] S. Eosoly, D. Brabazon, S. Lohfeld, L. Looney. Acta Biomater., 6 (2010), pp. 2511–2517

[30] N.E. Vrana, A. Elsheikh, N. Builles, O. Damour, V. Hasirci. Biomaterials, 28 (2007), pp. 4303–4310

[31] S. Eosoly, S. Lohfeld, D. Brabazon. in: M. Prado, C. Zavaglia (Eds.), Bioceramics, 21Trans Tech Publications Ltd, Stafa-Zurich (2009), pp. 659–662

[32] G. Ciapetti, L. Ambrosio, L. Savarino, D. Granchi, E. Cenni, N. Baldini, S. Pagani, S. Guizzardi, F. Causa, A. Giunti. Biomaterials, 24 (2003), pp. 3815–3824

[33] D.B. Burr. Bone, 31 (2002), pp. 8–11

[34] P. Garnero, O. Borel, E. Gineyts, F. Duboeuf, H. Solberg, M.L. Bouxsein, C. Christiansen, P.D. Delmas. Bone, 38 (2006), pp. 300–309

[35] C. Erisken, D.M. Kalyon, H. Wang. Biomaterials, 29 (2008), pp. 4065–4073

[36] M. Endres, D.W. Hutmacher, A.J. Salgado, C. Kaps, J. Ringe, R.L. Reis, M. Sittinger, A. Brandwood, J.T. Schantz. Tissue Eng.s, 9 (2003), pp. 689–702

[37] F. Causa, P.A. Netti, L. Ambrosio, G. Ciapetti, N. Baldini, S. Pagani, D. Martini, A. Giunti. J. Biomed. Mater. Res. Part A, 76A (2006), pp. 151–162

[38] A. Salerno, S. Zeppetelli, E. Di Maio, S. Iannace, P.A. Netti. Biotechnol. Bioeng., 108 (2011), pp. 963–976

[39] S.Z. Fu, X.H. Wang, G. Guo, S.A. Shi, M. Fan, H. Liang, F. Luo, Z.Y. Qian. J. Biomed. Mater. Res. Part B Appl. Biomater., 97B (2011), pp. 74–83

[40] D. Garcia-Alonso, M. Parco, J. Stokes, L. Looney. J. Therm. Spray Technol., 21 (2012), pp. 132–143

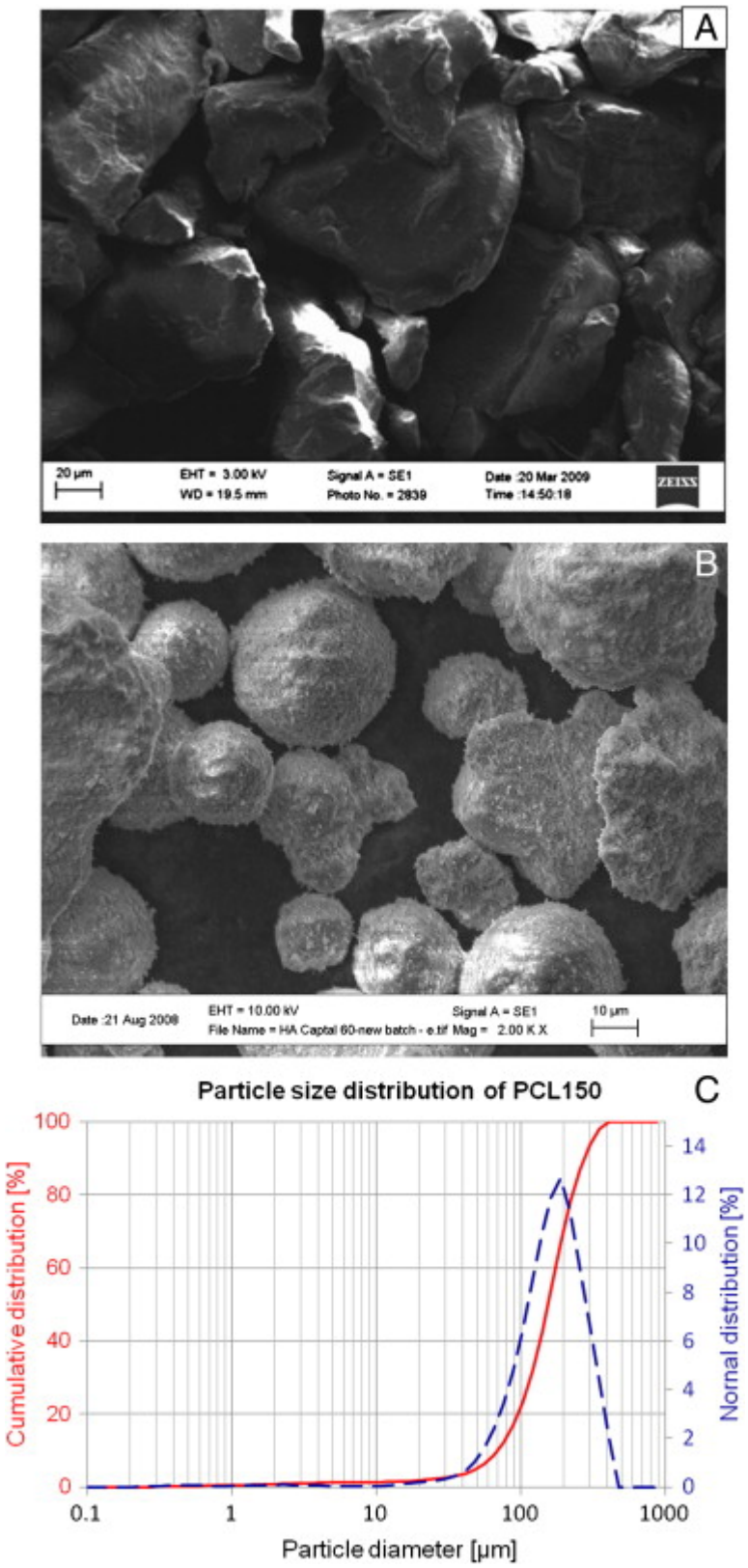

Fig. 1. (A) Morphology of the as-received powder ground by Solid Composites Ltd, (B) morphology of the as received HA powder, and (C) particle size distribution PCL100 powder ground by Solid Composites Ltd.

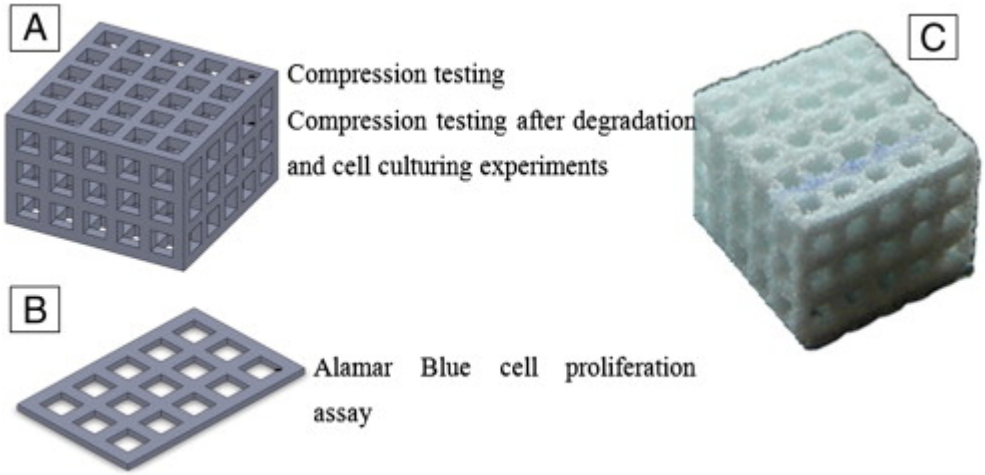

Fig. 2. (A) Geometry of 3D lattices designed for compression testing, (B) and of 2D lattices designed for performing Alamar blue cell proliferation assay, (C) fabricated 3D lattice structure.

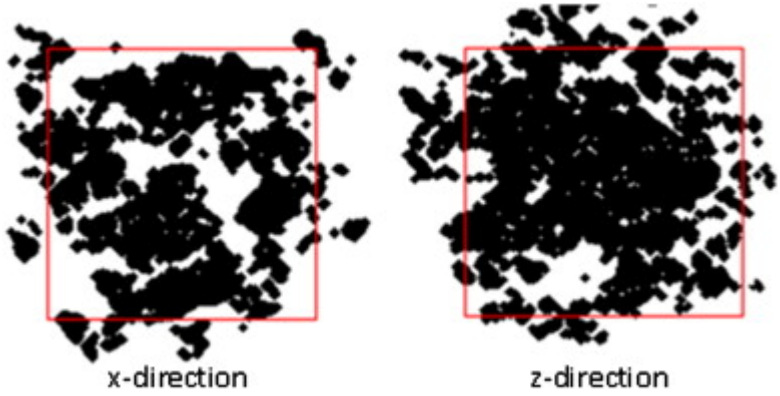

Fig. 3. Example cross-sections (x and z directions respectively) of scaffold struts derived from μ-CT data, the designed cross sectional area is superimposed on the image.

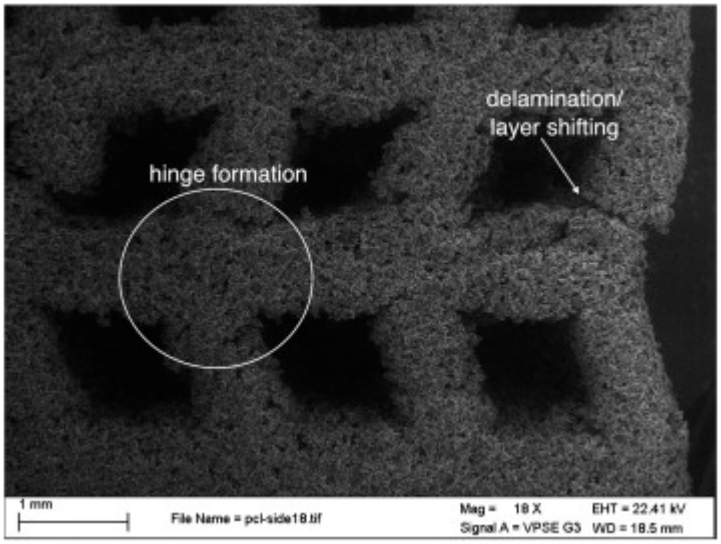

Fig. 4. SEM image of PCL scaffolds compressed along the load bearing (z) struts to strain below 25%.

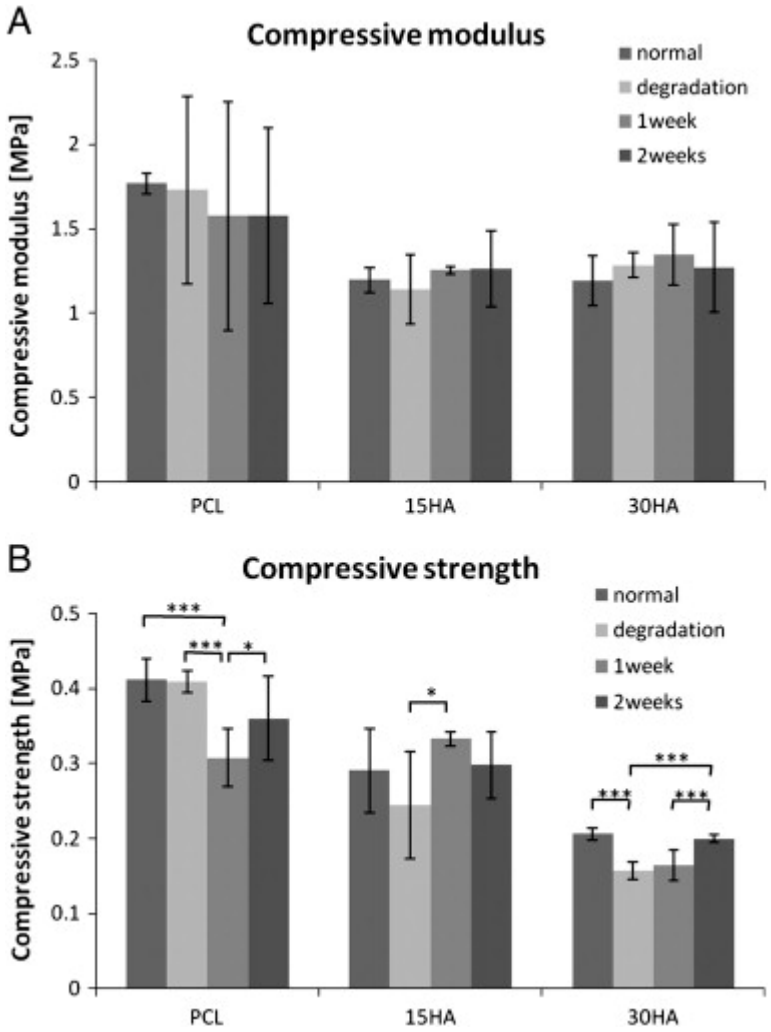

Fig. 5. (A) Effect of degradation tests and cell culturing on the compressive modulus of scaffolds, and (B) compressive strength of the scaffolds (*, ** and *** indicate significance at $p < 0.1$, $p < 0.05$ and $p < 0.01$, respectively), the "normal" sintered samples without degradation tests and cell culturing are included in the graphs as controls.

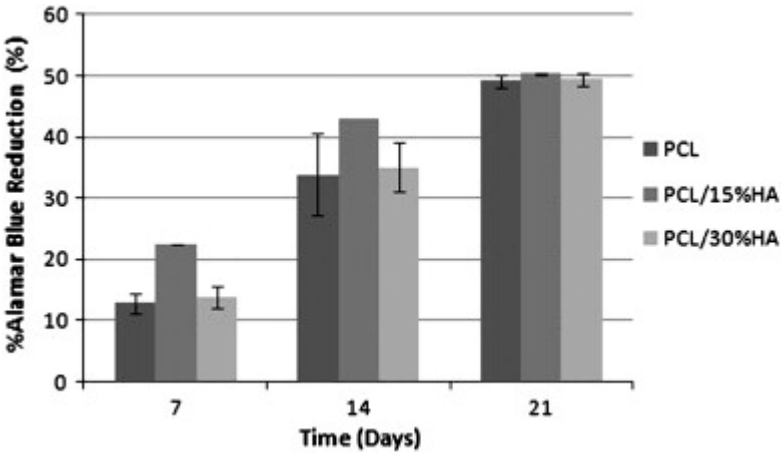

Fig. 6. Alamar blue assay for different compositions (PCL, PCL/15HA, PCL/30HA) after 7, 14 and 21 days of culturing.

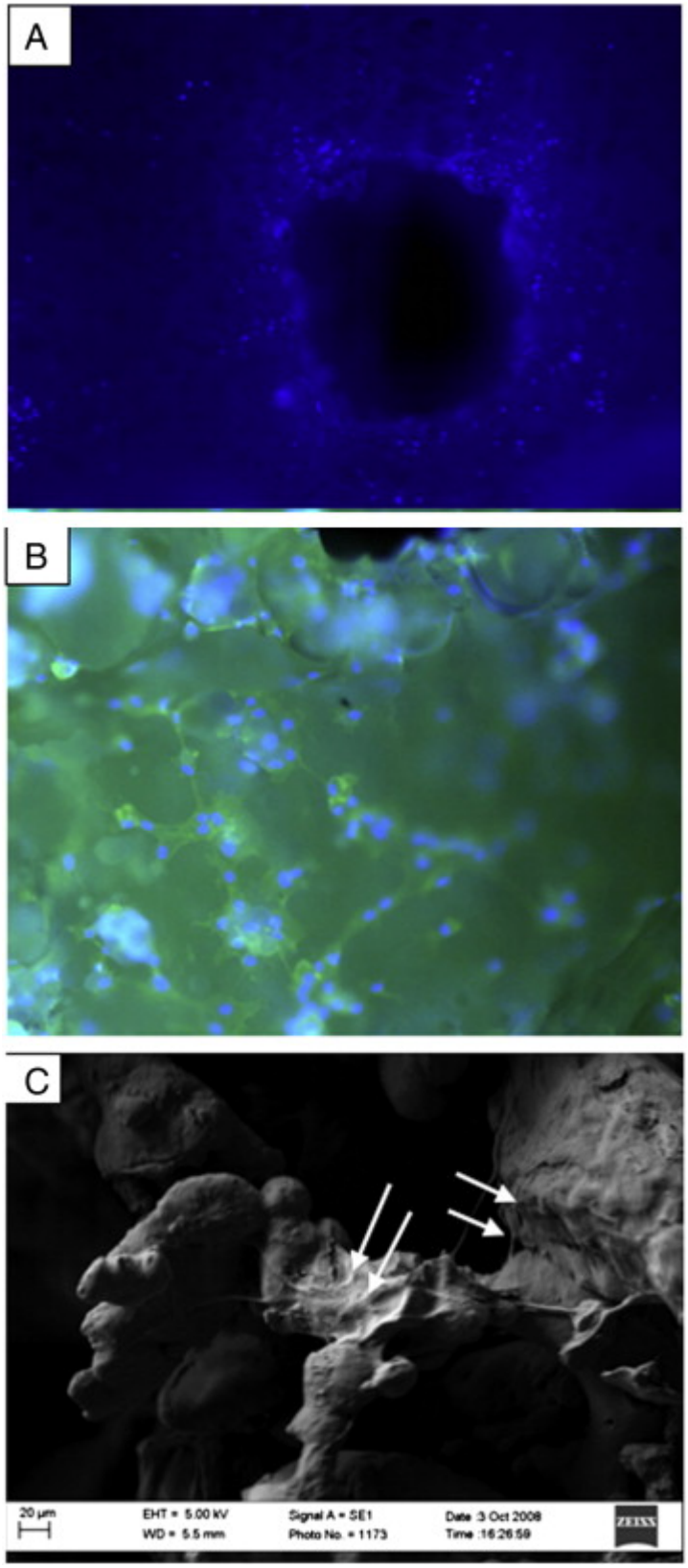

Fig. 7. (A) Concentration of cells close to the designed pores. (B) Well-spread cells within microporosities of PCL/15 wt.% HA scaffolds. (c) Presence of cells on PCL/15 wt.% HA scaffolds after 2 days of cell culturing (SEM).

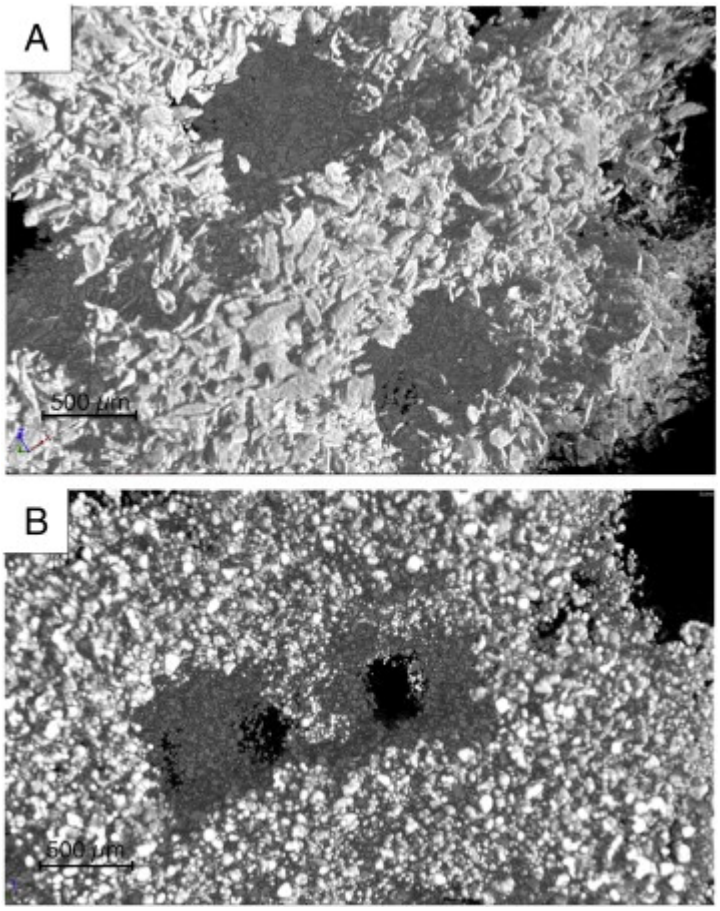

Fig. 8. (A) Struts of PCL scaffold reconstructed from µCT data. (B) Struts of cell seeded PCL scaffolds reconstructed from µCT data.

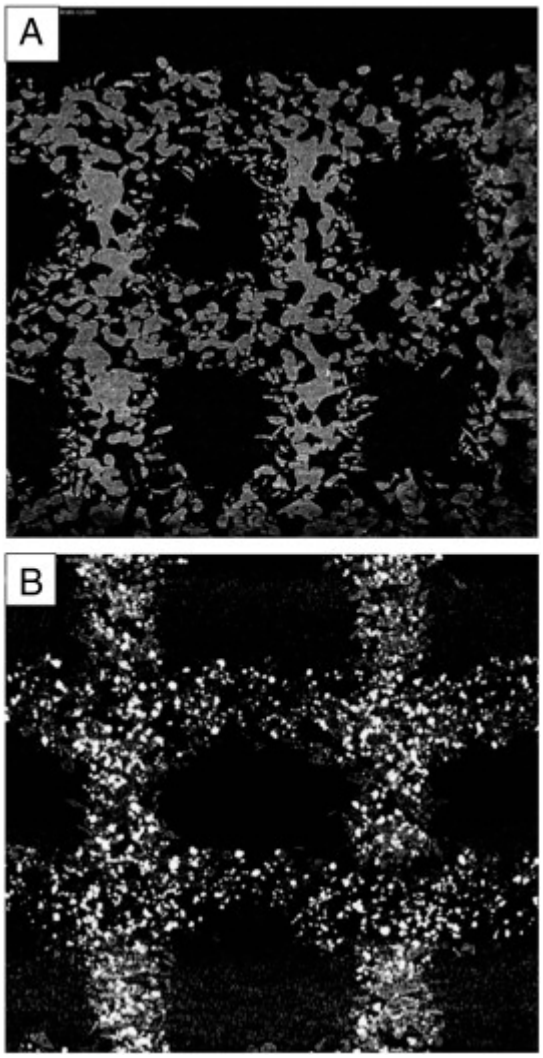

Fig. 9. Internal cross-section of (A) PCL scaffolds and (B) cell seeded PCL scaffolds from μCT data to demonstrate architectural and structural changes during cell culture conditions.

Table 1. Measured surface roughness values of solid disks with different material compositions.

Material	**Surface roughness—Ra [µm]**
PCL	33.24 ± 12.74
PCL/15HA	38.84 ± 12.83
PCL/30HA	32.47 ± 4.74